

## New variable transformations for evaluating nearly singular integrals in 2D boundary element method

Guizhong Xie, Jianming Zhang\*, Xianyun Qin, Guangyao Li

State Key Laboratory of Advanced Design and Manufacturing for Vehicle Body, College of Mechanical and Vehicle Engineering, Hunan University, Changsha 410082 China

### ARTICLE INFO

#### Article history:

Received 5 September 2010

Accepted 23 January 2011

#### Keywords:

Nearly singular integrals  
Numerical integration  
Boundary element method  
Variable transformation

### ABSTRACT

This work presents a further development of the distance transformation technique for accurate evaluation of the nearly singular integrals arising in the 2D boundary element method (BEM). The traditional technique separates the nearly hypersingular integral into two parts: a near strong singular part and a nearly hypersingular part. The near strong singular part with the one-ordered distance transformation is evaluated by the standard Gaussian quadrature and the nearly hypersingular part still needs to be transformed into an analytical form. In this paper, the distance transformation is performed by four steps in case the source point coincides with the projection point or five steps otherwise. For each step, new transformation is proposed based on the approximate distance function, so that all steps can finally be unified into a uniform formation. With the new formulation, the nearly hypersingular integral can be dealt with directly and the near singularity separation and the cumbersome analytical deductions related to a specific fundamental solution are avoided. Numerical examples and comparisons with the existing methods on straight line elements and curved elements demonstrate that our method is accurate and effective.

© 2011 Elsevier Ltd. All rights reserved.

### 1. Introduction

Near singularities are involved in many boundary element method (BEM) analyses of engineering problems, such as the thin and shell-like problems [1–3,6], the crack problems [7], the contact problems [8], as well as the sensitivity problems [9]. Accurate and efficient evaluation of nearly singular integrals is crucial for successful implementation of BEM analyses. A near singularity arises in BEM when a source point is close to but not on the integration elements. Although those integrals are really regular in nature, they cannot be evaluated accurately by the standard Gaussian quadrature. This is the so-called boundary layer effect in BEM. The boundary layer effect comes from the properties of fundamental solutions and their derivatives. The denominator, the distance between the source and the field point, is close to zero but not zero. The difficulty encountered in the numerical evaluation mainly results from the fact that the integrands of nearly singular integrals vary drastically with the distance.

Effective computation of nearly singular integrals has received intensive attention in recent years. Various numerical techniques have been developed to remove the near singularities, such as

rigid body displacement solutions [10], global regularization [4,5,11–14], semi-analytical or analytical integral formulas [15,16], the sinh transformation [17–19], polynomial transformation [20], adaptive subdivision method [21–23], distance transformation technique [24–27], the  $L_1^{-(1/5)}$  transformation [28] and the PART method [29]. Most of them benefit from the strategies for computing singular integrals. Among those techniques, the distance transformation technique seems to be a more promising method for dealing with different orders of nearly singular integrals. However, the traditional technique separates the nearly hypersingular integral into two parts with the aid of an introduced term having the similar hypersingular properties: a near strong singular part and a near hypersingular part. The near strong singular part with the one-ordered distance transformation can be evaluated by the standard Gaussian quadrature and the near hypersingular part still needs to be transformed into an analytical form. This is because the two distance transformations in Refs. [24–27] for the nearly hypersingular integral are not effective.

To cope with the above problems, a number of new transformations are introduced based on the approximate distance function to deal with the nearly hypersingular integral directly. Hence, the near singularity separation and the cumbersome formula deductions of the near hypersingular part in Refs. [24–27] are no longer required. We first take four steps to analyze the transformation when the distance between the source point and the projection point equals zero, and five steps otherwise. In each

\* Corresponding author. Tel.: +86 0731 88823061.

E-mail address: zhangjianm@gmail.com (J. Zhang).

step, the mathematical derivation is presented in detail. Then these steps are unified into a uniform formation, in which the near singularity separation and the cumbersome formula deductions can be avoided. It should be pointed out that we use the approximate distance but the exact distance in actual computation. Our method has been successfully applied in the evaluation of nearly singular integrals on straight line elements and curved elements. Numerical examples are presented for different cases regarding positions of the projection point and values of the minimum distance. Results demonstrate that our method is accurate and effective.

This paper is organized as follows. The general form of nearly singular integrals is described in Section 2. Section 3 briefly reviews the distance function. The distance transformations for near strong singular integrals are briefly reviewed in Section 4. In Section 5 the transformations for nearly hypersingular integrals are presented. Numerical examples are given in Section 6. The paper ends with conclusions in Section 7.

### 2. General descriptions

In this paper, we will deal with the computation of integrals of the following form:

$$I = \int_{\Gamma} \frac{f(x,y)}{r^l} d\Gamma, \quad l = 1, 2, \quad r = \|x-y\|_2 \quad (1)$$

where  $f$  is the smooth function,  $x$  and  $y$  represent the field point and the source point in BEM, respectively.  $\Gamma$  represents the boundary element. We assume that the source point is close to  $\Gamma$ , but not on it. In local intrinsic coordinate system,  $\xi \in [-1, 1]$ , the integrals of Eq. (1) can be transformed into the following forms:

$$\int_{\Gamma} \frac{f(x,y)}{r} d\Gamma = \int_{-1}^1 \frac{f(\xi)}{r} \phi(\xi) G(\xi) d\xi \quad (2a)$$

$$\int_{\Gamma} \frac{f(x,y)}{r^2} d\Gamma = \int_{-1}^1 \frac{f(\xi)}{r^2} \phi(\xi) G(\xi) d\xi \quad (2b)$$

where  $\phi(\xi)$  represents one of the shape functions, and  $G(\xi)$  is the Jacobian of the transformation from  $d\Gamma$  to  $d\xi$ .  $f(\xi)$ ,  $\phi(\xi)$  and  $G(\xi)$  are all the smooth functions.

Gaussians:  $\exp(-cr^2)$ ,  $c > 0$   
 Multiquadrics:  $(c^2 + r^2)^{-(\beta/2)}$ ,  $c \neq 0$

### 3. Review definition of the distance function

In this section, we will briefly review the distance function [24–27].

As shown in Fig. 1, employing the first-order Taylor expansion in the neighborhood of the projection point, we have

$$x_k - y_k = x_k - x_k^c + x_k^c - y_k = \frac{\partial x_k}{\partial \xi} \Big|_{\xi=c} (\xi - c) + r_0 n_k(c) + O(|\xi - c|^2) \quad (3)$$

where  $r_0$  is the minimum distance from the source point  $y$  to the

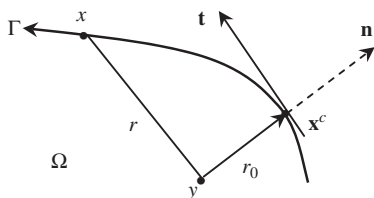


Fig. 1. The minimum distance  $r_0$ , from the source point to the 2D curved boundary element.

boundary element which is defined as the length of  $\overline{yx^c}$ ;  $t$  is the tangential line;  $x^c$  is the projection point and  $c$  is the local coordinate (see Fig. 1).

So the distance can be expanded to the following form:

$$\begin{aligned} r^2(\xi) &= (x_k - y_k)(x_k - y_k) \\ &= r_0^2 + \frac{\partial x_k}{\partial \xi} \frac{\partial x_k}{\partial \xi} \Big|_{\xi=c} (\xi - c)^2 + 2r_0 \frac{\partial x_k}{\partial \xi} \Big|_{\xi=c} n_k(c)(\xi - c) + O(|\xi - c|^3) \\ &= r_0^2 + G_c^2(\xi - c)^2 + G_c t_k(c) n_k(c)(\xi - c) + O(|\xi - c|^3) \\ &= G_c^2 g^2(\xi) + O(|\xi - c|^3) \end{aligned} \quad (4)$$

where  $G_c$  is the Jacobian at  $c$ ;  $n_k$  is the component of the outward normal and  $g(\xi)$  is the distance function defined as

$$g(\xi) = \sqrt{\alpha^2 + (\xi - c)^2} \quad (5)$$

where  $\alpha = r_0/G_c$

Consequently  $r$  can be expressed as

$$r = \sqrt{G_c^2 g^2(\xi)} \quad (6)$$

### 4. Variable transformations for near strong singular integrals

In this section, we review the distance transformation technique for near strong singularity with order  $1/r$ . There are two transformations considering the following two cases, namely  $r_0 \neq 0$  and  $r_0 = 0$ .

Case 1:  $r_0 \neq 0$ :

The following transformation pairs for the integration variables are given in Refs. [24–29] as

$$\eta(\xi) = \log[g(\xi) + (\xi - c)] \quad (7)$$

$$\xi(\eta) = \frac{1}{2}(e^\eta - \alpha^2 e^{-\eta}) + c \quad (8)$$

When  $|c| < 1$ , the integration span is split into two parts at point  $c$ . There is no need for this operation for the case  $|c| \geq 1$ . Substituting Eq. (8) into Eq. (2a) yields

$$\begin{aligned} \int_{\Gamma} \frac{f(x,y)}{r} d\Gamma &= \int_{-1}^1 \frac{f(\xi)}{r} \phi(\xi) G(\xi) d\xi \\ &= \int_{-1}^c \frac{f[\xi(\eta)]}{r} \phi[\xi(\eta)] G[\xi(\eta)] g[\xi(\eta)] d\eta \\ &\quad + \int_c^1 \frac{f[\xi(\eta)]}{r} \phi[\xi(\eta)] G[\xi(\eta)] g[\xi(\eta)] d\eta \end{aligned} \quad (9)$$

Case 2:  $r_0 = 0$ :

The following transformation for the integration variables has also been introduced in Refs. [27,28] as

$$\begin{cases} \xi(\eta) = e^\eta + c, & (c < -1) \\ \xi(\eta) = c - e^\eta, & (c > 1) \end{cases} \quad (10)$$

Using Eqs. (8) and (10), we can remove the near singularity with order  $1/r$  completely. The effectiveness for both transformations has also been verified by numerical examples in Refs. [24–29].

### 5. New variable transformations for nearly hypersingular integrals

In this section, we construct efficient variable transformations to compute nearly hypersingular integrals for different cases. Refs. [24–27] have given a transformation to remove this type near singularity completely in mathematical form, but the numerical results of the transformation are proved poorly. So it is time to developed new efficient transformations. Those transformations are based on the idea that the integrands with

the rapid variation are smoothed out and their integrals can be calculated precisely by the standard Gaussian quadrature. We will use different transformations for the following three cases: (1)  $r_0 \neq 0$  and  $|c| \geq 1$ ; (2)  $r_0 = 0$  and  $|c| \geq 1$ ; (3)  $r_0 \neq 0$  and  $|c| < 1$ .

### 5.1. Case 1: $r_0 \neq 0$ and $|c| \geq 1$

When  $r_0 \neq 0$  and  $|c| \geq 1$ , we will give different transformations considering the two ranges of  $c$ , namely  $c \leq -1$  and  $c \geq 1$ . In order to obtain a reasonable transformation for each case, the distance  $r$  is approximated by the Taylor expansion (4) without considering higher order term as Eq. (6). However, in actual computation  $r$  is still the distance from the source point to the field point. Taking the case  $c \leq -1$  as an example, we explain how to construct different transformations. The process consists of five steps and each step is described briefly below.

Using Eqs. (6) and (2b) can be written as

$$\begin{aligned} I &= \int_{-1}^1 \frac{f(\xi)}{r^2} \phi(\xi) G(\xi) d\xi = \int_{-1}^1 \frac{f(\xi)}{G_c^2 g^2(\xi)} \phi(\xi) G(\xi) d\xi \\ &= \int_{-1}^1 \frac{f(\xi)}{G_c^2 (\alpha^2 + (\xi - c)^2)} \phi(\xi) G(\xi) d\xi \end{aligned} \quad (11)$$

First we make a translation transformation for the integration variable as follows:

$$\xi_1 = \xi - c \quad (12)$$

Substituting Eq. (12) into (11) we have

$$\begin{aligned} I &= \int_{-1}^1 \frac{f(\xi)}{r^2} \phi(\xi) G(\xi) d\xi = \int_{-1-c}^{1-c} \frac{f(\xi_1 + c)}{G_c^2 g^2(\xi_1 + c)} \phi(\xi_1 + c) G(\xi_1 + c) d\xi_1 \\ &= \int_{-1-c}^{1-c} \frac{f(\xi_1 + c)}{(r_0^2 + G_c^2 \xi_1^2)} \phi(\xi_1 + c) G(\xi_1 + c) d\xi_1 \end{aligned} \quad (13)$$

Second we make a stretching transformation

$$\xi_1 = r_0 \xi_2 \quad (14)$$

Eq. (13) becomes the following form:

$$I_1 = \int_{-(1+c)/r_0}^{(1-c)/r_0} \frac{r_0 f(r_0 \xi_2 + c)}{(r_0^2 + G_c^2 r_0^2 \xi_2^2)} \phi(r_0 \xi_2 + c) G(r_0 \xi_2 + c) d\xi_2 \quad (15)$$

In the third steps we make a translation transformation again

$$\xi_3 = \xi_2 + 1 \quad (16)$$

This step is employed to adjust the lower limit of the integration variable for the afterward logarithmic transformation.

Substituting Eq. (16) into Eq. (15), results in

$$I = \int_{-(1+c)/r_0+1}^{((1-c)/r_0)+1} \frac{r_0 f[r_0(\xi_3-1)+c]}{(r_0^2 + G_c^2 r_0^2 (\xi_3-1)^2)} \phi(r_0(\xi_3-1)+c) G(r_0(\xi_3-1)+c) d\xi_3 \quad (17)$$

In the fourth steps, we smooth out the rapid variations of the integrand by the following logarithmic transformation:

$$\xi_4 = \log(\xi_3) \quad (18)$$

Eq. (17) can be expressed as

$$\begin{aligned} I &= \int_{\log(-(1+c)/r_0)+1}^{\log((1-c)/r_0)+1} \frac{r_0 e^{\xi_4} f[r_0(e^{\xi_4}-1)+c]}{(r_0^2 + G_c^2 r_0^2 (e^{\xi_4}-1)^2)} \\ &\quad \times \phi(r_0(e^{\xi_4}-1)+c) G(r_0(e^{\xi_4}-1)+c) d\xi_4 \end{aligned} \quad (19)$$

Using the good properties of the logarithmic function [24–30], it can easily be proved that the transformed integrand has much lower gradient.

Finally, adjusting the integration interval within  $[-1, 1]$  for performing the standard Gaussian quadrature directly, we propose the following transformation:

$$\xi_4 = k_1 \eta + k_2 \quad (20)$$

where

$$\begin{cases} k_1 = 0.5 \left( \log\left(\frac{1-c}{r_0} + 1\right) - \log\left(\frac{-1-c}{r_0} + 1\right) \right) \\ k_2 = 0.5 \left( \log\left(\frac{1-c}{r_0} + 1\right) + \log\left(\frac{-1-c}{r_0} + 1\right) \right) \end{cases} \quad (21)$$

Using the transformation (20), we have

$$\begin{aligned} I &= \int_{-1}^1 \frac{k_1 r_0 e^{k_1 \eta + k_2} f(r_0(e^{k_1 \eta + k_2} - 1) + c)}{(r_0^2 + G_c^2 r_0^2 (e^{k_1 \eta + k_2} - 1)^2)} \\ &\quad \times \phi(r_0(e^{k_1 \eta + k_2} - 1) + c) G(r_0(e^{k_1 \eta + k_2} - 1) + c) d\eta \end{aligned} \quad (22)$$

We integrate all the transformations detailed above and can obtain the final transformation as

$$\xi = c + r_0(e^{k_1 \eta + k_2} - 1) \quad (23)$$

Using Eq. (23), the integral of Eq. (2b) can be expressed as follows:

$$\begin{aligned} I &= \int_{-1}^1 \frac{k_1 r_0 e^{k_1 \eta + k_2} f(r_0(e^{k_1 \eta + k_2} - 1) + c)}{r^2} \\ &\quad \times \phi(r_0(e^{k_1 \eta + k_2} - 1) + c) G(r_0(e^{k_1 \eta + k_2} - 1) + c) d\eta \end{aligned} \quad (24)$$

It should be noted that we still use the exact  $r$  instead of the approximate  $r$  in Eq. (24) and the nearly singular kernels are not changed into another forms.

For the case  $c \geq 1$ , in a similar manner, we can easily obtain another new transformation as follows:

$$\xi = c - r_0(e^{k_1 \eta + k_2} - 1) \quad (25)$$

where  $k_1$  and  $k_2$  are different from those in Eq. (21), both values are obtained using the following equations:

$$\begin{cases} k_1 = 0.5 \left( \log\left(\frac{1+c}{r_0} + 1\right) - \log\left(\frac{c-1}{r_0} + 1\right) \right) \\ k_2 = 0.5 \left( \log\left(\frac{1+c}{r_0} + 1\right) + \log\left(\frac{c-1}{r_0} + 1\right) \right) \end{cases} \quad (26)$$

Using Eq. (25), the integral of Eq. (2b) for this case can be expressed as follows:

$$\begin{aligned} I &= \int_{-1}^1 \frac{k_1 r_0 e^{k_1 \eta + k_2} f(c - r_0(e^{k_1 \eta + k_2} - 1))}{r^2} \\ &\quad \times \phi(c - r_0(e^{k_1 \eta + k_2} - 1)) G(c - r_0(e^{k_1 \eta + k_2} - 1)) d\eta \end{aligned} \quad (27)$$

### 5.2. Case 2: $r_0 = 0$ and $|c| \geq 1$

When  $r_0 = 0$  and  $|c| > 1$ , the process of constructing variable transformations is different from that described in Section 5.1. We also deduce corresponding transformations for the two cases, namely  $c \leq -1$  and  $c \geq 1$ . Taking the case  $c \leq -1$  as an example, the process consisting of four steps is described briefly below.

Using Eqs. (6) and (2b) can be transformed into the following form:

$$\begin{aligned} I &= \int_{-1}^1 \frac{f(\xi)}{r^2} \phi(\xi) G(\xi) d\xi = \int_{-1}^1 \frac{f(\xi)}{G_c^2 g^2(\xi)} \phi(\xi) G(\xi) d\xi \\ &= \int_{-1}^1 \frac{f(\xi)}{G_c^2 (\xi - c)^2} \phi(\xi) G(\xi) d\xi \end{aligned} \quad (28)$$

First we still make a translation transformation

$$\xi_1 = \xi - c \quad (29)$$

Eq. (28) becomes the following form:

$$I = \int_{-1-c}^{1-c} \frac{1}{G_c^2 \xi_1^2} \phi(\xi_1 + c) G(\xi_1 + c) d\xi_1 \quad (30)$$

Second we make a stretching transformation

$$\xi_1 = (-1-c)\xi_2 \tag{31}$$

The integral of Eq. (30) can be written as

$$I = \int_{-1}^{(1-c)/-(1+c)} \frac{-(1+c)}{(1+c)^2 \xi_2^2} \phi(-(1+c)\xi_2+c)G(-(1+c)\xi_2+c)d\xi_2 \tag{32}$$

Third we make a logarithmic transformation to smooth out the rapid variations of the integrand

$$\xi_3 = \log(\xi_2) \tag{33}$$

Using Eq. (33), we have

$$I = \int_0^{\log((1-c)/-(1+c))} \frac{-(1+c)e^{\xi_3}}{(1+c)^2 (e^{\xi_3})^2} \times \phi(-(1+c)e^{\xi_3}+c)G(-(1+c)e^{\xi_3}+c)d\xi_3 \tag{34}$$

Finally, also adjusting the interval of integration within  $[-1,1]$  for performing the standard Gaussian quadrature directly, the following transformation is given:

$$\xi_3 = k(\eta+1), \quad k = 0.5\log\left(\frac{1-c}{-1-c}\right) \tag{35}$$

Substituting Eq. (35) into Eq. (34), we have

$$I = \int_{-1}^1 \frac{-(1+c)ke^{k(1+\eta)}}{(1+c)^2 (e^{k(1+\eta)})^2} \times \phi(-(1+c)e^{k(1+\eta)}+c)G(-(1+c)e^{k(1+\eta)}+c)d\eta \tag{36}$$

We integrate all steps above and the final transformation is obtained as

$$\xi = c+(-1-c)e^{k(1+\eta)} \tag{37}$$

Applying the transformation described by Eq. (37), the integral of Eq. (2b) for this case can be expressed as follows:

$$I = \int_{-1}^{-1} \frac{(-1-c)ke^{k(1+\eta)}}{r^2} \times \phi(c+(-1-c)(e^{k(1+\eta)}-1))G(c+(-1-c)(e^{k(1+\eta)}-1))d\eta \tag{38}$$

For the case  $c \geq 1$ , after applying the similar processes we can easily obtain another new transformation as follows:

$$\xi = c-(c-1)(e^{k(1+\eta)}-1), \quad k = 0.5\log((1+c)/(c-1)) \tag{39}$$

Using Eq. (39), the integral of Eq. (2b) for this case can be expressed as follows:

$$I = \int_{-1}^1 \frac{(c-1)ke^{k(1+\eta)}}{r^2} \times \phi(c-(c-1)(e^{k(1+\eta)}-1))G(c-(c-1)(e^{k(1+\eta)}-1))d\eta \tag{40}$$

### 5.3. Case 3: $r_0 \neq 0$ and $|c| < 1$

If  $r_0 \neq 0$  and  $|c| < 1$ , we split the integration span into two parts at point  $c$ , Eq. (2b) can be expressed with two parts as

$$I = \int_{-1}^c \frac{f(\xi)}{r^2} \phi(\xi)G(\xi)d\xi = I_1 + I_2 \tag{41}$$

in which

$$I_1 = \int_c^1 \frac{f(\xi)}{r^2} \phi(\xi)G(\xi)d\xi \tag{42a}$$

$$I_2 = \int_{-1}^c \frac{f(\xi)}{r^2} \phi(\xi)G(\xi)d\xi \tag{42b}$$

Employing the similar method detailed in the previous subsections, we can construct an efficient variable transformation for each part.

For Eq. (42a), the following variable transformation is given:

$$\xi = c+r_0(e^{k(1+\eta)}-1), \quad k = 0.5\log\left(\frac{1-c}{r_0}+1\right) \tag{43}$$

Substituting Eq. (43) into Eq. (42a), yields

$$I_1 = \int_{-1}^1 \frac{r_0ke^{k(1+\eta)}f(c+r_0(e^{k(1+\eta)}-1))}{r^2} \times \phi(c+r_0(e^{k(1+\eta)}-1))G(c+r_0(e^{k(1+\eta)}-1))d\eta \tag{44}$$

For Eq. (42b), we can also obtain the following transformation:

$$\xi = c-r_0(e^{k(1+\eta)}-1), \quad k = 0.5\log\left(\frac{1+c}{r_0}+1\right) \tag{45}$$

Substituting Eq. (45) into Eq. (42b), results in

$$I_2 = \int_{-1}^1 \frac{r_0ke^{k(1+\eta)}f[c-r_0(e^{k(1+\eta)}-1)]}{r^2} \times \phi(c-r_0(e^{k(1+\eta)}-1))G(c-r_0(e^{k(1+\eta)}-1))d\eta \tag{46}$$

Note that the two variable transformations are similar to Ref. [30]. However, the deductions in this paper are very different from than those given in Ref. [30]. We construct the transformations in a general way based on the approximate distance function derived from first-order Taylor expansion. The effectiveness for both transformations has also been verified by numerical examples in Ref. [30].

## 6. Numerical examples

In this section, we will give a number of examples to investigate the effectiveness of different variable transformations. For the purpose of error estimation, the relative error is defined as follows:

$$error = \left| \frac{I_{nume} - I_{exact}}{I_{exact}} \right| \tag{47}$$

where the subscripts *nume* and *exact* refer to numerical solutions and exact solutions, respectively.

### 6.1. Numerical examples of straight line elements

In this section, numerical examples of straight elements are given to verify the effectiveness of the proposed transformations. We use 10 Gaussian points in all cases for the convenience of comparison.

#### Example 1.

$$\int_{-1}^1 \frac{1}{(c-x)^2} dx = \frac{1}{c-1} - \frac{1}{c+1} \tag{48}$$

This example considers the nearly singular integrals of the left side of Eq. (48). The projection point is located outside the integration interval and the minimum distance equals zero, namely  $r_0=0$  and  $|c| \geq 1$ . The relative distance describing the closeness of the source point to the boundary is defined as

$$ratio = \left| \frac{c-1}{2} \right| \tag{49}$$

The integrals of the left side of Eq. (48) are computed considering the different values of  $c$ .  $c$  changes from 1.1 to 1.000001. The solutions of our method are obtained with the transformation of Eq. (39). And exact solutions are obtained by the right side of Eq. (48). We will compare our method with Telles' method [20]. The results and the relative errors are listed in Tables 1 and 2.

**Table 1**Comparisons of numerical results between our method and Telles' method ( $r_0=0$  and  $|c| \geq 1$ ).

Ratio	Exact solution	Our method	Telles' second degree method	Telles' third degree method
0.5e-01	9.523809523809520	9.523809523809502	9.52380592265220	9.5238095094771040
0.5e-02	99.50248756218906	99.50248756218880	99.2822207439216	99.500172446645564
0.5e-03	999.5002498750624	999.5002498751232	885.260216571448	995.33053859668246
0.5e-04	9999.500024998750	9999.500024956229	4336.74536591694	9234.9679996985451
0.5e-05	99999.50000184488	99999.49998902746	9628.00429700836	63785.179740187421
0.5e-06	999999.5000825167	999999.4982712528	13101.0132970434	264763.92332233913

**Table 2**Comparisons of relative errors between our method and Telles' method ( $r_0=0$  and  $|c| \geq 1$ ).

Ratio	Errors of our method	Errors of Telles' second degree method	Errors of Telles' third degree method
0.5e-01	1.8652e-15	3.7812e-07	1.5049e-09
0.5e-02	2.5707e-15	2.2136e-03	2.3267e-05
0.5e-03	6.0853e-14	0.114297153320266	4.1718e-03
0.5e-04	4.2523e-12	Wrong	7.6457e-02
0.5e-05	1.2817e-10	Wrong	Wrong
0.5e-06	1.8000e-09	Wrong	Wrong

Another example has been presented in [20] as

$$I = \int_{-1}^1 \frac{1}{(1.004-x)^2} dx = 249.500998003992$$

The application of Telles' second degree method to the above integral gives  $I=245.59074481306968$  (an error of 1.6 percent) and the application of Telles' third degree method gives  $I=249.43489486343037$  (an error of 0.026 percent). Using our transformation of Eq. (39) to the same integral gives  $I=249.50099800399101$  (an error of  $4.0e-15$ , more accurate than Telles' method).

From Tables 1 and 2 and the example above, it should be noted that Telles' method is stable and accurate when  $ratio > 0.5e-04$ , especially Telles' third degree method. But when  $ratio < 0.5e-04$ , Telles' method fails. Compared with Telles' method, our method is more accurate and stable in all cases. It is clearly found that the results with our method are very accurate with the relative errors less than  $10^{-8}$  even ratio set to  $0.5e-06$ .

It is also pointed out that this case appears in many BEM models such as employing discontinuous linear elements. This example has shown our method can deal with integrals of this type accurately and efficiently.

**Example 2.**

$$\int_{-1}^1 \frac{1}{(c-x)^2 + r_0^2} dx = \frac{1}{r_0} \arctan\left(\frac{1-c}{r_0}\right) - \frac{1}{r_0} \arctan\left(\frac{-1-c}{r_0}\right) \quad (50)$$

In this example, the coordinate  $c$  of the projection point is outside the integration interval and the minimum distance is not equal to zero, namely  $r_0 \neq 0$  and  $|c| \geq 1$ . The relative distance describing the closeness of the source point to the boundary is defined as

$$ratio = \left| \frac{\sqrt{(c-1)^2 + r_0^2}}{2} \right| \quad (51)$$

$r_0$  changes from 0.1 to 0.000001 by the order  $10^{-1}$  and  $c$  changes from 1.1 to 1.000001. Using our transformation (25), the integrals can easily be computed by the standard Gaussian quadrature. The solutions with our method are obtained with the transformation of Eq. (25). And exact solutions are obtained by the right side of Eq. (50). We will also compare this example with Telles'

method [20]. The results are listed in Table 3 and the relative errors are listed in Table 4.

From Tables 3 and 4, it is found that the largest error of our method is less than 0.08 percent even ratio set to  $0.714e-06$ . It should be noted that Telles' method is stable and accurate when  $ratio > 0.714e-04$ , especially Telles' third degree method. However, when  $ratio < 0.714e-04$ , Telles' method fails. Compared with Telles' method, our method is more accurate and stable for all cases. It should be noted that these integrals cannot be calculated accurately with the traditional distance transformation technique directly, while very accurate results have been obtained with our transformation easily.

**6.2. Numerical examples of curved elements**

In this section, numerical examples on curved elements are presented to verify the effectiveness of the proposed transformations. We use 20 Gaussian points in all cases for the convenience of comparison. Numerical examples are computed over a quadratic boundary element with the nodal coordinates (0,0.5), (1,1), (2,1). We consider the integrals with near hyper singularity ( $q_k^i$ ) as follows:

$$q_1^i = \int \frac{1}{r^2} \left( 2r_1 \frac{\partial r}{\partial n} - n_1 \right) \phi_i d\Gamma, \quad i = 1, 2, 3 \quad (52)$$

where  $n$  represents the unit normal;  $x$  is the field point and  $y$  is the source point,  $r_1 = x_1 - y_1$ ,  $r_2 = x_2 - y_2$ ,  $\partial r / \partial n = (r_1 n_1 + r_2 n_2) / r$ ;  $\phi_i$  is one of the shape functions.

**Example 3.**

$$q_1^i = \int \frac{1}{r^2} \left( 2r_1 \frac{\partial r}{\partial n} - n_1 \right) \phi_i d\Gamma, \quad i = 1, 2, 3$$

In this example we consider the positions of the projection point for two cases. The relative distance describing the closeness of the nearly singular point to the boundary is defined as

$$ratio = \frac{\sqrt{(y_1-2)^2 + (y_2-1)^2}}{l} \quad (53)$$

where  $l$  is the length of the curved element, and  $(y_1, y_2)$  is the source point. And exact solutions are obtained by adaptive subdivision method [21–23]. We divide the curved element into many sub-elements, and for each sub-element, 10 Gaussian points are used. But for our method, only 20 Gaussian points are employed on the whole element.

For the first case, the coordinate  $c$  of the projection point is outside the integration interval and the minimum distance is not equal to zero, namely  $r_0 \neq 0$  and  $|c| \geq 1$ .  $r_0$  changes from 0.1 to 0.000001 by the order  $10^{-1}$  and  $c$  changes from 1.2 to 1.000002. And the source point  $(y_1, y_2)$  moves along the normal line  $\bar{y}\bar{n}$  through the projection point  $c$ . While accurate computation of those integrals cannot be performed by the distance transformation technique directly, the near singularity separation and the cumbersome formula deductions are still required. Using our transformation (25), the integrals can easily be computed by the

**Table 3**Comparisons of numerical results between our method and Telles' method ( $r_0 \neq 0$  and  $|c| \geq 1$ ).

Ratio	Exact solution	Our method	Telles' second degree method	Telles' third degree method
0.714e-01	7.37815060120465	7.3781506112580630	7.3781541301331668	7.3781504305069827
0.714e-02	78.04230800665944	78.042295418995295	78.134460267067169	78.032054798911048
0.714e-03	784.8984133141152	784.87437917911507	778.58781833389685	789.14904182114219
0.714e-04	7853.481658973651	7852.8638064086572	4273.6432633693794	8047.1885742484974
0.714e-05	78539.31634191728	78546.524751965859	9623.6783375383566	61722.1402401590970
0.714e-06	785397.6634388316	785988.371264560730	13100.923425304798	263978.995513185100

**Table 4**Comparisons of relative errors between our method and Telles' method ( $r_0 \neq 0$  and  $|c| \geq 1$ ).

Ratio	Errors of our method	Errors of Telles' second degree method	Errors of Telles' third degree method
0.714e-01	1.3626e-09	4.7829e-07	2.3136e-08
0.714e-02	1.6129e-07	1.18086e-03	1.3138e-04
0.714e-03	3.0621e-05	8.0400e-03	5.4155e-03
0.714e-04	7.8672e-05	0.455828198377955476	2.4665e-02
0.714e-05	9.1781e-05	Wrong	-0.214124299587042
0.714e-06	7.5211e-04	Wrong	Wrong

**Table 5**Comparisons of relative errors between our method and Ma's method ( $\phi_i = \phi_1$ ,  $r_0 \neq 0$  and  $|c| \geq 1$ ).

Ratio	6.14e-02	7.29e-03	7.42e-04	7.44e-05	7.44e-06	7.44e-07
Exact solution	-0.3287745755301	-0.296079663522	-0.1457373223479	0.0338550865416	0.2174935543268	0.4016330570280
Errors						
Our method	7.100e-9	8.603e-7	4.660e-5	1.700e-3	1.700e-3	2.619e-5
Ma's	1.658e-8	2.821e-5	1.300e-3	8.86e-2	1.52e-2	1.84e-2

**Table 6**Relative errors of our method and Ma's method ( $\phi_i = \phi_2$ ,  $r_0 \neq 0$  and  $|c| \geq 1$ ).

Ratio	6.14e-02	7.29e-03	7.42e-04	7.44e-05	7.44e-06	7.44e-07
Exact solution	0.145981897672	0.291858543852	0.891701987414	1.610305220541	2.344926996697	3.081496270124
Errors						
Our method	6.219e-8	3.599e-6	1.8274e-5	1.606e-4	2.524e-04	3.894e-4
Ma's	3.789e-7	1.052e-4	6.5017e-4	3.900e-3	2.900e-3	1.33e-2

**Table 7**Relative errors of our method and the standard Gaussian quadrature ( $\phi_i = \phi_1$ ,  $r_0 = 0$  and  $|c| \geq 1$ ).

Ratio	1.26e-01	1.18e-02	1.17e-03	1.17e-04	1.17e-05	1.17e-06
Exact solution	-0.354376509579	-0.34718 586787	-0.207607028191	-0.031156631298	0.151936187522	0.336003048354
Errors						
Our method	4.416e-9	1.165e-6	6.260e-5	3.400e-3	1.800e-3	1.700e-3
Gau-quad	1.304e-7	6.300e-3	3.900e-2	Wrong	Wrong	Wrong

standard Gaussian quadrature. The solutions with our method are obtained with the transformation of Eq. (25). We compare our new method with Ma's method [24–27]. The relative errors are listed in Tables 5 and 6. In this example we only compute integrals of Eq. (52) when  $i=1, 2$ .

From Tables 5 and 6, it is found that the largest error of our method is less than 0.04 percent even the ratio set to  $7.44e-07$ . Compared with Ma's method, it should be noted that while Ma's method is accurate and stable even when the ratio is very small, the near singularity separation and the cumbersome formula deductions cannot be avoided. Using our method, the integrals can be computed directly additional transformation. Moreover, our method is more accurate and stable.

For the second case, we consider the projection point is located outside the integration interval and the minimum distance equals

zero, namely  $r_0=0$  and  $|c| \geq 1$ . We assume that  $c$  changes from 1.2 to 1.000002 by the order  $10^{-1}$ . The results are obtained with our method and the standard Gaussian quadrature, respectively. For all cases, 20 Gaussian points is used on the whole element. Relative errors are listed in Tables 7 and 8. The symbol *Gau-quad* denotes the results obtained with the standard Gaussian quadrature.

Since the distance between the source point and (2,1) is very small compared with the length of the integration element, the integrals become nearly hypersingular. The solutions of our method are obtained with the transformation of Eq. (39). We will compare the results of our new transformation with the exact solutions. The relative errors are listed in Tables 7 and 8. We also consider  $i=1, 2$ , respectively.

From Tables 7 and 8, it is found that when  $ratio < 1.18e-02$ , the standard Gaussian quadrature fails.

**Table 8**Relative errors of our method and the standard Gaussian quadrature ( $\phi_i = \phi_2$ ,  $r_0 = 0$  and  $|c| \geq 1$ ).

Ratio	1.26e-01	1.18e-02	1.17e-03	1.17e-04	1.17e-05	1.17e-06
Exact solution	-0.21702373784	0.052052048880	0.639835580787	1.349724798153	2.082634448863	2.818968950858
Errors						
Our method	8.953e-16	5.967e-6	1.817e-5	2.229e-04	4.477e-05	1.000e-3
Gau-quad	7.773e-7	16.71e-2	Wrong	Wrong	Wrong	Wrong

But our method is more accurate and stable even ratio set to  $1.17e-06$ . The largest error of our method is less than 0.2 percent for all cases.

## 7. Conclusion

Several new variable transformations are presented in this paper for accurate computation of nearly singular integrals arising in 2D BEM. The goal of developing those transformations is to overcome the drawbacks of the traditional distance transformation technique.

The new variable transformations are based on the distance function and each for different cases in terms of the minimum distance and the positions of the projection point. These transformations are finally unified into a uniform formulation, which can deal with the nearly hypersingular integral directly, and thus the near singularity separation and cumbersome formula deductions in traditional methods are avoided.

The accuracy and efficiency of the method is verified by a number of numerical examples and compared with the existing methods. It has been found that our method is more stable and accurate. The relative errors of our new transformations can be kept within  $10^{-3}$  up till  $ratio = 10^{-6}$ . Moreover, our method has been applied in the evaluation of nearly singular integrals on straight line elements and curved elements as a general algorithm. Extension of our method to 3D BEM is an ongoing work.

## Acknowledgments

This work was supported in part by National 973 Project of China under Grant no. 2010CB328005, in part by National Science Foundation of China under Grant no. 10972074.

## References

- [1] Cruse TA, Aithal R. Non-singular boundary integral equation implementation. *Int J Numer Methods Eng* 1993;36:237–54.
- [2] Liu YJ. Analysis of shell-like structures by the boundary element method based on 3-D elasticity: formulation and verification. *Int J Numer Methods Eng* 1998;41:541–58.
- [3] Krishnasamy G, Rizzo FJ, Liu YJ. Boundary integral equations for thin bodies. *Int J Numer Methods Eng* 1994;37:107–21.
- [4] Zhang JM, Yao ZH. Meshless regular hybrid boundary node method. *Comput Modeling Eng Sci* 2001;2:307–18.
- [5] Zhang JM, Yao ZH, Tanaka M. The meshless regular hybrid boundary node method for 2-D linear elasticity. *Eng Anal Bound Elem* 2003;27:259–68.
- [6] Zhang JM, Yao ZH. Analysis of 2-D thin structures by the meshless regular hybrid boundary node method. *Acta Mech Solida Sinica* 2002;15:36–44.
- [7] Dirgantara T, Aliabadi MH. Crack growth analysis of plates loaded by bending and tension using dual boundary element method. *Int J Fatigue* 2000;105:27–47.
- [8] Aliabadi MH, Martin D. Boundary element hypersingular formulation for elasto-plastic contact problems. *Int J Numer Methods Eng* 2000;48:995–1014.
- [9] Zhang D, Rizzo FJ, Rudolph TJ. Stress intensity sensitivities via hypersingular boundary integral equations. *Comput Mech* 1999;23:389–96.
- [10] Chen HB, Lu P, Huang MG, Williams FW. An effective method for finding values on and near boundaries in the elastic BEM. *Comput Struct* 1998;69:421–31.
- [11] Sladek N, Sladek J, Tanaka M. Regularization of hypersingular and nearly singular integrals in the potential theory and elasticity. *Int J Numer Methods Eng* 1993;36:1609–28.
- [12] Liu YJ, Rudolph TJ. New identities for fundamental solutions and their applications to non-singular boundary element formulations. *Comput Mech* 1999;24:286–92.
- [13] Liu YJ. On the simple solution and non-singular nature of the BIE/BEM—a review and some new results. *Eng Anal Bound Elem* 2000;24:789–95.
- [14] Krishnasamy G, Schmerr LW, Rudolph TJ, Rizzo FJ. Hypersingular boundary integral equations: some applications in acoustic and elastic wave scattering. *J Appl Mech* 1990;57:404–14.
- [15] Niu ZR, Wendland WL, Wang XX, Zhou HL. A sim-analytic algorithm for the evaluation of the nearly singular integrals in three-dimensional boundary element methods. *Comput Methods Appl Mech Eng* 2005;31:949–64.
- [16] Zhou HL, Niu ZR, Cheng CZ, Guan ZW. Analytical integral algorithm applied to boundary layer effect and thin body effect in BEM for anisotropic potential problems. *Comput Struct* 2008;86:1656–71.
- [17] Johnston Peter R, Elliott David. A sinh transformation for evaluating nearly singular boundary element integrals. *Int J Numer Methods Eng* 2005;62:564–78.
- [18] Johnston Barbara M, Johnston Peter R, Elliott David. A sinh transformation for evaluating two-dimensional nearly singular boundary element integrals. *Int J Numer Methods Eng* 2007;69:1460–79.
- [19] Elliott David, Johnston Peter R. Error analysis for a sinh transformation used in evaluating nearly singular boundary element integrals. *J Comput Appl Math* 2007;203:103–24.
- [20] Tells JCF. A self adaptive coordinate transformation for efficient numerical evaluations of general boundary element integrals. *Int J Numer Methods Eng* 1987;24:959–73.
- [21] Zhang JM, Qin XY, Han X, Li GY. A boundary face method for potential problems in three dimensions. *Int J Numer Methods Eng* 2009;80:320–37.
- [22] Qin XY, Zhang JM, Li GY, et al. An element implementation of the boundary face method for 3D potential problems. *Eng Anal Bound Elem* 2010;34:934–43.
- [23] Gao XW, Davies TG. Adaptive integration in elasto-plastic boundary element analysis. *J Chin Inst Eng* 2000;23:349–56.
- [24] Ma H, Kamiya N. A general algorithm for the numerical evaluation of nearly singular boundary integrals of various orders for two- and three-dimensional elasticity. *Comput Mech* 2002;29:277–88.
- [25] Ma H, Kamiya N. A general algorithm for accurate computation of field variables and its derivatives near boundary in BEM. *Eng Anal Bound Elem* 2001;25:833–41.
- [26] Ma H, Kamiya N. Distance transformation for the numerical evaluation of near singular boundary integrals with various kernels in boundary element method. *Eng Anal Bound Elem* 2002;26:329–39.
- [27] Ma H, Kamiya N. Nearly singular approximations of CPV integrals with end and corner-singularities for the numerical solution of hypersingular boundary integral equations. *Eng Anal Bound Elem* 2003;27:625–37.
- [28] Hayami K, Matsumoto H. A numerical quadrature for nearly singular boundary element integrals. *Eng Anal Bound Elem* 1994;13:143–54.
- [29] Hayami K. Variable transformations for nearly singular integrals in the boundary element method. 41. Kyoto University: Publications of Research Institute for Mathematical Sciences; 2005. p. 821–42.
- [30] Zhang YM, Gu Y, Chen JT. Boundary layer effect in BEM with high order geometry elements using transformation. *Comput Modeling Eng Sci* 2009;45:227–47.